

Tuning dehydrogenation temperature of carbon–ammonia borane nanocomposites†

Saghar Sepehri, Betzaida B. Garcia and Guozhong Cao*

Received 20th May 2008, Accepted 18th July 2008

First published as an Advance Article on the web 30th July 2008

DOI: 10.1039/b808511k

The effect of pore size on dehydrogenation temperature and kinetics of coherent carbon–ammonia borane nanocomposites prepared by sol–gel synthesis as potential on-board hydrogen storage materials is reported.

Hydrogen storage is a key issue in hydrogen technology; considerable efforts have been made in synthesizing and investigating novel materials for hydrogen storage in the past decade.¹ Although various techniques and materials have been used and/or studied to store hydrogen, there is neither method nor material that satisfies all the requirements of perceived hydrogen economy.² Ideally, hydrogen should be stored in the form of a liquid or solid so as to attain high storage capacity, under near the ambient conditions to be safe and economical, and perform rapid and reversible hydrogenation and dehydrogenation process for practical applications.

Physisorption of hydrogen in highly porous media, such as activated carbon, is an attractive approach since the physisorption process is perfectly reversible and rapid, but it requires high pressure and suffers from relatively low storage capacity.^{3–5} Hydrides are a group of materials that offer high storage capacity at ambient conditions. However, they suffer from other drawbacks, such as poor reversibility in chemical hydrides, low storage capacity in metal hydrides, poor thermal conductivity, and relatively high and un-tunable dehydrogenation temperatures.⁶

Development of new hydrides, particularly complex hydrides, has been a very active research topic.⁷ Admixing amides into hydrides and/or introducing sufficient catalytic compounds have been demonstrated to be efficient approaches to reducing the dehydrogenation temperature through altering reaction pathways.^{8,9} Nanostructured hydrides have shown an enhanced rate of hydrogen desorption and absorption.¹⁰ Confining hydrides inside nanoporous scaffolds has been demonstrated to be an effective approach to tune the hydrogen storage properties. For example, the dehydrogenation temperature of ammonia borane (AB) was reduced when confined inside the pores of mesoporous silica.¹¹ The same effect was found when ammonia borane and lithium borohydride were impregnated inside nanoporous carbon.^{12,13}

The ability to tune the dehydrogenation temperature of hydrides is of great interest in developing hydrogen materials. In this Communication, we report that the dehydrogenation temperatures of ammonia borane can be tuned by controlling the pore size of the porous scaffold in coherent carbon–AB nanocomposites and our work has demonstrated a direct relationship: smaller pores leads to lower dehydrogenation temperatures, and lower activation energies.

Carbon cryogels (CC) with different pore sizes were derived from resorcinol–formaldehyde hydrogels through controlled pyrolysis.^{14,15} CC–AB nanocomposites were made by loading monolithic CCs with AB through soaking them in AB–THF solution,¹² the total weight gain of the samples was between 30–50 wt% (which is 1 : 2 to 1 : 1 by weight ratio for AB : CC).‡ Cross-sectional SEM micrographs of cryogels (Fig. 1) show the microstructure before and after loading with AB and also after the dehydrogenation. CC has an interconnected network (Fig. 1a), soaking CC in an AB–THF solution results in distribution of AB within the CC scaffold (Fig. 1b). After dehydrogenation, the porous structure of CC is sustained and a fiber-like residue of AB is scattered throughout the CC (Fig. 1c).

The coherent CC–AB nanocomposites consist of nanocrystallite AB dispersed and confined in the CC matrix as shown by X-ray diffraction (XRD) analysis (Fig. 2). Using Sherrer's method¹⁶ the approximate crystallite size for AB in CC–AB is calculated as 25 ± 4 nm. Splitting of the (110) and (101) peaks was observed in CC–AB, which can be attributed to broadening as a result of small crystallite sizes for AB in CC and possible strain from the composites.¹⁷

Nitrogen sorption analysis was used to study the porous structure of CCs and CC–ABs and showed that the CC samples are mesoporous (with pore sizes of 2–50 nm), with BET surface areas of 350–500 m² g⁻¹, and total pore volumes of 0.69–0.97 cm³ g⁻¹. The pore size distributions (PSDs) were obtained by applying the BJH method on the desorption curve of the BET isotherms.¹⁸ Fig. 3 (left) shows the PSD of three CC samples with pore diameters centered at ~7, 9, and 16 nm, respectively. The changes in the PSD of the 7nm CC when loaded with AB (CC–AB), and after dehydrogenation (reacted) are

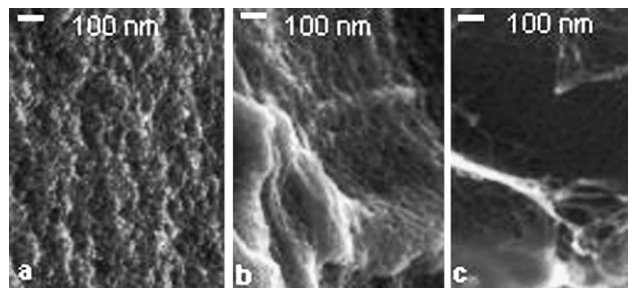


Fig. 1 SEM images of (a) CC, (b) CC–AB, (c) reacted CC–AB.

Department of Materials Science and Engineering, University of Washington, Box 352120, Seattle, WA 98195-2120, USA. E-mail: gzcao@u.washington.edu; Fax: +1-206-543-3100

† The pore structure of carbon cryogels was analyzed by means of nitrogen sorption (BET technique) at -196 °C using a Quantachrome NOVA 4200e instrument. Dehydrogenation studies were performed using a Netzsch 200 differential scanning calorimeter. X-Ray diffraction measurements were taken with a Siemens D5000 using the $K\alpha_1$ line of a copper source, $\lambda = 1.54184$ Å, for standard θ – 2θ scans on well-ground samples.

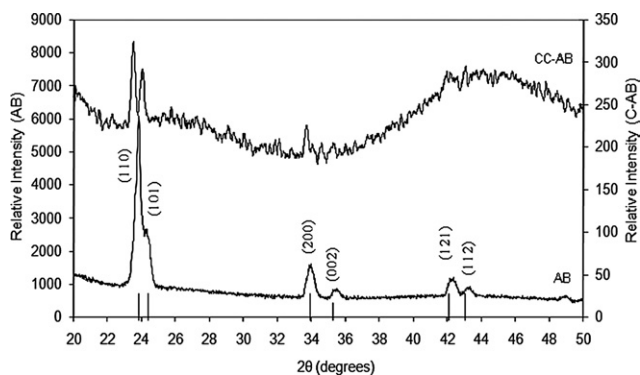


Fig. 2 XRD pattern for neat AB (below) and powdered CC-AB nanocomposite (above), shows AB in the amorphous carbon cryogel.

shown in Fig. 3 (right). Loading CCs with AB fills some of the mesopores resulting in an appreciable reduction in pore volume and a shift in PSD towards smaller pore sizes (7.5 nm \rightarrow 6.5 nm), which can be indicative of uniform loading of AB throughout the CCs. The porous structure of the CC is maintained after thermal reaction, dehydrogenation partially emptied some of the filled pores and increased pore volume but PSD did not show appreciable shift. §

It also revealed that the higher AB loading corresponded to the samples with higher pore volumes. Using the pore volume of the CCs, their weight gain, and density of AB, it was calculated that up to 90% of the CC free space was filled with AB.

Dehydrogenation reactions were studied using differential scanning calorimetry (DSC). At the preliminary runs, the CC-AB nanocomposites were heated to 200 °C in dry argon at a heating rate of 5 °C min⁻¹. The DSC exotherms for CC-ABs and neat AB are given in Fig. 4. Thermal decomposition of neat AB happens through two step reactions which at the heating rate used are observed at approximately 115 and 150 °C, and are in good agreement with the literature.¹⁹ For the CCs with pore sizes of 7, 9, and 16 nm, dehydrogenation temperatures are much lower than that of neat AB (at ~98, 102, and 110 °C, respectively) and hydrogen release happens through only one exothermic event. Lower dehydrogenation temperatures in CC-ABs provide evidence for faster kinetics. The dehydrogenation of nanocomposites is very reproducible and, as we

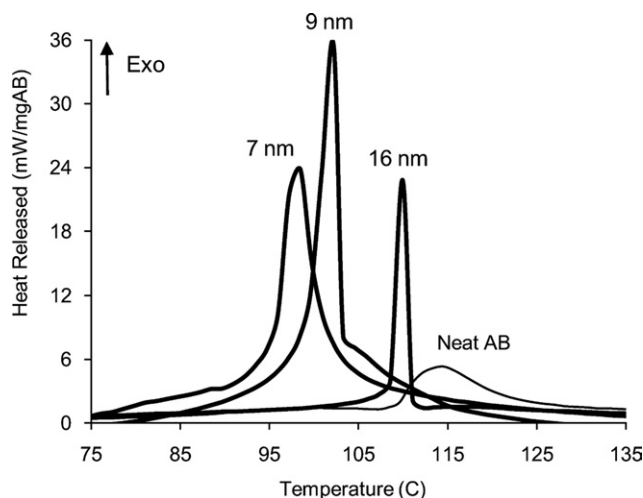


Fig. 4 DSC exotherms for CC-AB nanocomposites (at 5 °C min⁻¹).

reported before, results in the release of about 1.5 H₂ equiv. suppression of borazine, and shows a significantly higher reaction exothermicity than that of neat AB.¹² Also, our previous study using ¹¹B nuclear magnetic resonance and Fourier transform infrared spectroscopy (FTIR) showed that the lower dehydrogenation temperature and enhanced kinetics in the thermal reaction of CC-AB are accompanied by the formation of a new reaction product that is assigned to reaction of AB with surface oxygen functional groups.²⁰

Fig. 4 also shows that the dehydrogenation for CC-ABs occurs over a much narrow range of temperatures than for neat AB. Although the exact mechanism for narrowed dehydrogenation peaks is under research, it is likely to be due to the better thermal conductivity of the nanocomposites and the consequently more rapid kinetics as compared to the neat AB.

The peak dehydrogenation of CC-ABs and their corresponding CC pore size are compared in Fig. 5, the solid line connecting the peak temperatures shows the direct relationship between the dehydrogenation temperature and the pore size.

The activation energies for 7 nm and 16 nm CC-ABs, were calculated by non-isothermal DSC runs at multiple heating rates, using the Kissinger equation,²¹ which is given by:

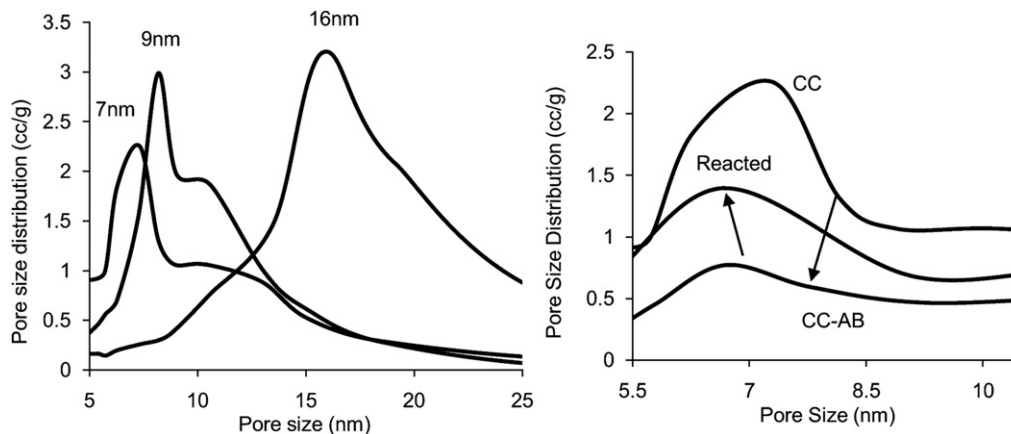


Fig. 3 Pore size distributions of CCs used for making CC-AB nanocomposites, as determined by the BJH method on the desorption curve of nitrogen sorption isotherms (left), and pore size distribution of the 7 nm CC and CC-AB nanocomposite before and after dehydrogenation (right).

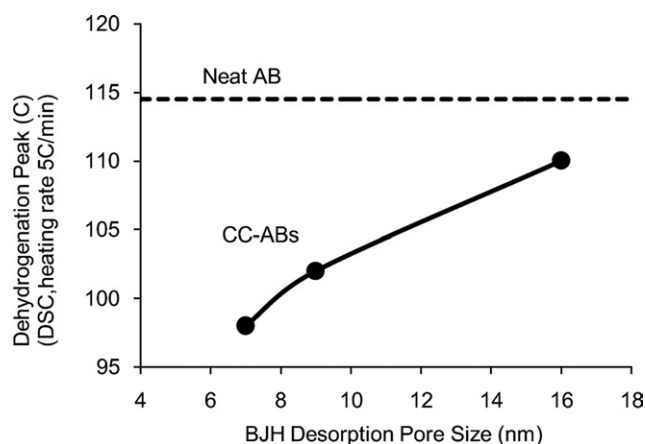


Fig. 5 Comparison of dehydrogenation peaks for CC-AB nanocomposites for corresponding CC pore sizes, the solid line connects the data points for visual guidance. The dashed line shows the dehydrogenation temperature for AB at similar heating rate ($5\text{ }^{\circ}\text{C min}^{-1}$).

$$\ln(\alpha/T_p^2) = -E_a/RT_p + \text{int}$$

where T_p is the peak temperature, $\alpha = dT/dt$ is the heating rate, E_a is the activation energy, and int is the intercept. The plot of $\ln(\alpha/T_p^2)$ versus $1/T_p$ is linear and the slope of the resulting line corresponds to the values of activation energy from the Kissinger equation.

The peak temperatures for heating rates of 2, 5, and $10\text{ }^{\circ}\text{C min}^{-1}$, and the calculated activation energies are given in Table 1. Three different runs were performed at each rate, and the observed peak temperatures occurred in general at reproducible temperatures with less than $1\text{ }^{\circ}\text{C}$ difference. The dehydrogenation temperatures and the activation energies for nanocomposites are lower than that of neat AB. The activation energy for neat AB is about 160 kJ mol^{-1} , which is comparable to the reported value using the isothermal method,¹¹ and that of 16 nm CC-AB and 7 nm CC-AB are about 150 kJ per molAB and 120 kJ per molAB, respectively.

Similar to the dehydrogenation temperatures, the activation energies decrease with decreasing pore size. The corresponding Kissinger plots are given in Fig. 6, which shows that the slope of 7 nm CC-AB (activation energy) is quite different of the other two lines, while the slope of 16 nm CC-AB is close to that of neat AB. This observation can be because of the larger pores in the latter, and suggests that the barrier for hydrogen release for CC-ABs decreases with pore size.

In summary, this study shows the direct dependence of the dehydrogenation temperature and kinetics of ammonia borane on pore size in amorphous nanoporous carbon-ammonia borane nanocomposites. These materials have a coherent design, all the parts involved are coordinated harmoniously to enhance the hydrogen

Table 1 Peak temperatures for dehydrogenation of AB and CC-AB

Heating rate/ $^{\circ}\text{C min}^{-1}$	AB	16 nm CC-AB	7 nm CC-AB
	$T_p/^{\circ}\text{C}$	$T_p/^{\circ}\text{C}$	$T_p/^{\circ}\text{C}$
10	124	115	109
5	118	109	101
2	112	103	94
E_a	160 kJ mol^{-1}	150 kJ mol^{-1}	120 kJ mol^{-1}

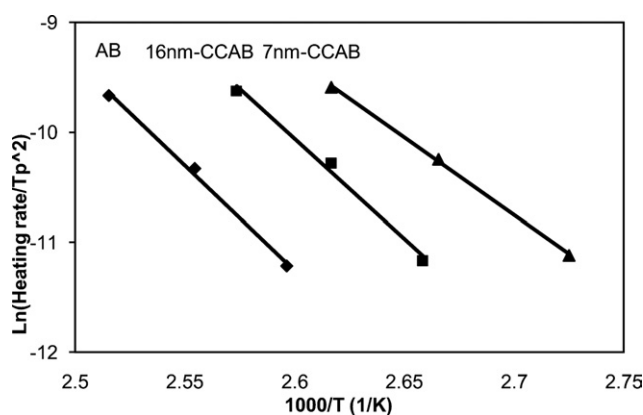


Fig. 6 Kissinger plots for non-isothermal DSC runs at heating rates of 2, 5, and $10\text{ }^{\circ}\text{C min}^{-1}$. Activation energies are calculated from the slopes.

storage properties; the interconnected porous carbon network with large pore volume and surface area acts as the host to the hydride and also as a structure-directing agent, reduces the hydrogen diffusion distances, increases the frequency of reaction which effectively accelerates the dehydrogenation process, and serves as an efficient pathways for heat transfer. Inside the mesopores of the CC matrix, nanocrystallite AB possesses a huge surface to volume ratio, resulting in a significantly larger surface energy, and thus destabilizing the hydrogen bonding network of AB and lowering the barrier to hydrogen release. We are currently studying other possible factors (such as surface area and catalysts) on dehydrogenation temperatures to gain a better control over the dehydrogenation temperature. Increasing the surface area may enhance the surface interaction and result in lower dehydrogenation temperatures. Also, a parallel research is ongoing to tune the surface chemistry of CCs and study the destabilization effects of doped CCs on the dehydrogenation.

Acknowledgements

Support for this work was provided by the National Science Foundation (DMR-0605159), WTC, and EnerG2 LLC.

Notes and references

‡ Sample weight gain % = (weight of CC-AB – weight of CC)/ weight of CC-AB.

§ For CC, CC-AB, and reacted CC-AB, the BET surface area was measured at 500, 120, and $250\text{ m}^2\text{ g}^{-1}$, and BJH desorption cumulative pore volumes were 0.69, 0.13, and 0.31 cc g^{-1} , respectively.

- S. Satyapal, J. Petrovic, C. Read, G. Thomas and G. Ordaz, *Catal. Today*, 2007, **120**, 246.
- S. Orimo, Y. Nakamori, J. R. Eliseo, A. Züttel and C. M. Jensen, *Chem. Rev.*, 2007, **107**, 4111.
- M. Fichtner, *Scr. Mater.*, 2007, **56**, 801.
- H. Kabbour, T. F. Baumann, J. H. Satcher, A. Saulnier and C. C. Ahn, *Chem. Mater.*, 2006, **18**, 6085.
- M. Jordá-Beneyto, F. Suárez-García, D. Lozano-Castelló, D. Cazorla-Amorós and A. Linares-Solano, *Carbon*, 2007, **45**, 293.
- A. M. Seayad and D. M. Antonelli, *Adv. Mater.*, 2004, **16**, 765.
- A. Züttel, P. Wenger, P. Sudan, P. Mauron and S. Ormio, *Mater. Sci. Eng.*, 2004, **B108**, 9.
- W. Grochala and P. P. Edwards, *Chem. Rev.*, 2004, **104**, 1283.
- E. Rönnebro and E. H. Majzoub, *J. Phys. Chem.*, 2006, **B110**, 25686.

-
- 10 C. P. Baldé, B. P. C. Hereijgers, J. H. Bitter and K. P. de Jong, *Angew. Chem.*, 2006, **45**, 1.
 - 11 A. Gutowska, L. Li, Y. Shin, C. M. Wang, X. H. S. Li, J. C. Linehan, R. S. Smith, B. D. Kay, B. Schmid, W. Shaw, M. Gutowski and T. Autrey, *Angew. Chem., Int. Ed.*, 2005, **44**, 3578.
 - 12 A. M. Feaver, S. Sepehri, P. Shamberger, A. Stowe, T. Autrey and G. Z. Cao, *J. Phys. Chem. B*, 2007, **111**, 7469.
 - 13 A. F. Gross, J. J. Vajo, S. L. Van Atta and G. L. Olson, *J. Phys. Chem. C*, 2008, **112**, 5651.
 - 14 R. W. Pekala, *J. Mater. Sci.*, 1989, **24**, 3221.
 - 15 H. Tamon, H. Ishizaka, T. Yamamoto and T. Suzuki, *Carbon*, 1999, **37**, 2049.
 - 16 C. Suryanarayana, M. Grant Norton, *X-Ray Diffraction: A Practical Approach*, Plenum Press, New York and London, 1998.
 - 17 B. Palsoz, S. Stelmakh, E. Grzanka, S. Gierlotka, R. Pielaszek, U. Bismayer, S. Werner and W. Palosz, *J. Phys.: Condens. Matter*, 2004, **16**, S353.
 - 18 M. Thommes, *Nanoporous Materials: Science and Engineering*, ed. G. Q. Lu, X. S. Zhao, Imperial College Press, London, 2004, vol. 4.
 - 19 F. Baitalow, J. Baumann, G. Wolf, K. Jaenicke-Rößler and G. Leitner, *Thermochim. Acta*, 2002, **391**, 159.
 - 20 S. Sepehri, A. M. Feaver, W. J. Shaw, C. J. Howard, Q. Zhang, T. Autrey and G. Z. Cao, *J. Phys. Chem. B*, 2007, **111**, 14285.
 - 21 H. E. Kissinger, *Anal. Chem.*, 1957, **11**, 1702.